Life Sciences 248 (2020) 117477

Contents lists available at ScienceDirect

Life Sciences

journal homepage: www.elsevier.com/locate/lifescie

Anti-HCV, nucleotide inhibitors, repurposing against COVID-19

Abdo A. Elfiky*

Biophysics Department, Faculty of Sciences, Cairo University, Giza, Egypt
College of Applied Medical Sciences, University of Al-Jouf, Saudi Arabia

ARTICLE INFO

Keywords:
Wuhan coronavirus
COVID-19
RdRp
Docking
Structural bioinformatics
Sofosbuvir
Nucleotide inhibitors

ABSTRACT

Aims: A newly emerged Human Coronavirus (HCoV) is reported two months ago in Wuhan, China (COVID-19). Until today > 2700 deaths from the 80,000 confirmed cases reported mainly in China and 40 other countries. Human to human transmission is confirmed for COVID-19 by China a month ago. Based on the World Health Organization (WHO) reports, SARS HCoV is responsible for > 8000 cases with confirmed 774 deaths. Additionally, MERS HCoV is responsible for 858 deaths out of about 2500 reported cases. The current study aims to test anti-HCV drugs against COVID-19 RNA dependent RNA polymerase (RdRp).
Materials and methods: In this study, sequence analysis, modeling, and docking are used to build a model for Wuhan COVID-19 RdRp. Additionally, the newly emerged Wuhan HCoV RdRp model is targeted by anti-polymerase drugs, including the approved drugs Sofosbuvir and Ribavirin.
Key findings: The results suggest the effectiveness of Sofosbuvir, IDX-184, Ribavirin, and Remidisvir as potent drugs against the newly emerged HCoV disease.
Significance: The present study presents a perfect model for COVID-19 RdRp enabling its testing *in silico* against anti-polymerase drugs. Besides, the study presents some drugs that previously proved its efficiency against the newly emerged viral infection.

1. Introduction

A new emerged human coronavirus (COVID-19) is reported in December 2019 in Wuhan, China [1,2]. According to the World Health Organization (WHO) surveillance draft in January 2020, any traveler to Wuhan, Hubei Province in China, two weeks before the onset of the symptoms, is suspected to be a COVID-19 patient [1,3]. Additionally, WHO distributed interim guidance for laboratories that carry out the testing for the newly emerged outbreak and infection prevention and control guidance [4,5]. COVID-19 viral pneumonia is related to the seafood market when an unknown animal is responsible for the emergence of the outbreak [2]. Other countries started their surveillance borders to prevent the spread of the new unknown coronavirus [6]. Until one month ago, 41 cases were confirmed to be COVID-19 positives leaving one dead and seven in critical care in China. This number is grossly increasing daily, and the number of confirmed cases at the date of writing this manuscript exceeded 80,000, with > 2700 deaths [7–9[63]]. On 20 January 2020, the National Health Commission of China confirmed the human-to-human transmission of the Wuhan outbreak (COVID-19) [9]. The symptoms include fever, malaise, dry cough, shortness of breath, and respiratory distress [2].

COVID-19 is a member of *Betacoronaviruses* like the Severe Acute Respiratory Syndrome Human coronavirus (SARS HCoV) and the Middle-East Respiratory Syndrome Human coronavirus (MERS HCoV) [10,11]. Until today, six different strains of Human coronaviruses (HCoVs) have been reported, in addition to the newly emerged COVID-19 [2,12]. 229E and NL63 strains of HCoVs belong to *Alphacoronaviruses* while OC43, HKU1, SARS, MERS, and COVID-19 HCoVs belong to *Betacoronaviruses* [2,11]. SARS and MERS HCoV are the most aggressive strains of coronaviruses, leaving about 800 deaths each. SARS HCoV has a 10% mortality rate, while MERS HCoV has a 36% mortality rate, according to the WHO [11–15].

HCoVs generally are positive-sense and very long (30,000 bp) single-stranded RNA viruses. Two groups of protein characterize HCoVs; structural, such as Spike (S), Nucleocapsid (N) Matrix (M) and Envelope (E), and non-structural proteins such as RNA dependent RNA polymerase (RdRp) (nsp12) [11]. RdRp is a crucial enzyme in the life cycle of RNA viruses, including coronaviruses. RdRp is targeted in different RNA viruses, including Hepatitis C Virus (HCV), Zika Virus (ZIKV), and coronaviruses (CoVs) [16–24]. The active site of RdRp is highly conserved representing two successive aspartate residues protruding from a beta-turn structure making them surface accessible through the nucleotide channel (free nucleotides can pass through) [25,26].

* Biophysics Department, Faculty of Sciences, Cairo University, Giza, Egypt.
E-mail addresses: abdo@sci.cu.edu.eg, aelfiky@ictp.it.

https://doi.org/10.1016/j.lfs.2020.117477
Received 27 January 2020; Received in revised form 26 February 2020; Accepted 26 February 2020
Available online 28 February 2020

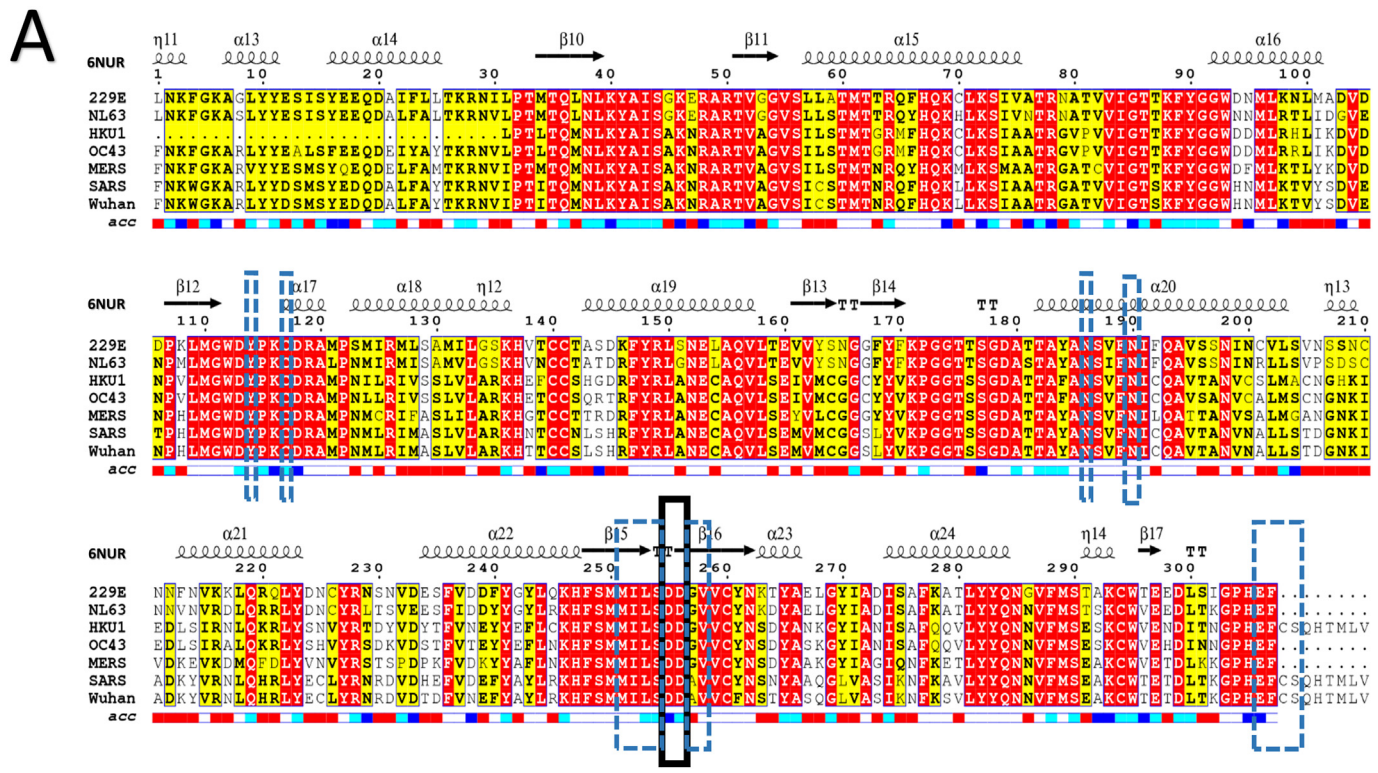

Fig. 1. (A) Multiple sequence alignment of all the HCoV strains (229E, NL63, HKU1, OC43, MERS, SARS, and COVID-19) RdRp sequences. Red highlights indicate identical residues while yellow highlighted residues are less conserved. Secondary structures are represented at the top of the MSA for SARS RdRp (PDB ID: 6NUR, chain A), while the surface accessibility is shown at the bottom (blue: highly accessible while white is buried). The black dashed rectangles mark active site aspartates while blue rectangles mark the residues lying in the 5 Å region surrounding the active aspartates. The alignment is made using the Clustal omega web server and represented by ESpript 3. (B) The newly emerged COVID-19 RdRp model built by Swiss Model in the green cartoon (right) and surface (left) representations. Two views of the polymerase at 180° rotation on the horizontal plane are shown (top and bottom). The active site aspartates are represented in red sticks for clarification (see the enlarged panel). (C) Ramachandran plot for the COVID-19 RdRp model. (For interpretation of the references to color in this figure legend, the reader is referred to the web version of this article.)

Several *in vitro* and clinical trials started in China during the last month with the first approved drug, Favilavir, by the National Medical Products Administration of China is announced yesterday (18 February 2020) in Zhejiang province. Different directly acting antiviral drugs are approved against other viruses, by the Food and Drugs Administration (FDA), such as Sofosbuvir, Ribavirin against RdRp of Hepatitis C Virus (HCV). These drugs are nucleotides derivative competing with physiological nucleotide for RdRp active site [22,27,28]. Additionally, a huge number of attempts to develop anti-RdRp compounds are under clinical testing against different viruses. The half-maximal Effective Concentration (EC50) for Ribavirin against COVID-19 is 109.5 μM, while its half-maximum Inhibition Concentration (IC50) against Dengue virus is 8 μM [29,30]. Sofosbuvir show 4 μM against the Zika virus [31]. Remdesivir shows EC90 of 1.76 μM against COVID-19 *in vitro* [30]. We focus here in the present study on nucleotide inhibitors due to its strong evidence of inhibiting emerging viral RdRps [11,16]. We build the COVID-19 RdRp model using homology modeling after sequence comparison to the available structures in the protein data bank [32]. Molecular docking is then performed to test some direct-acting antiviral (DAA) drugs against COVID-19 RdRp (Sofosbuvir, Ribavirin, Remidisvir, IDX-184). Additionally, the native nucleotides GTP and UTP, from which IDX-184 and Sofosbuvir are derived, are also tested against COVID-19 RdRp model. The results are promising and suggest possible inhibition for the currently available therapeutics against the newly emerged coronavirus.

2. Materials and methods

2.1. Sequence alignment and modeling

The first available full genome sequence for the newly emerged COVID-19 (NC_045512.2) is retrieved from the National Center for Biotechnology Information (NCBI) nucleotide database [33]. Swiss Model web server is used to build a model for RdRp using its automated mode [34]. SARS HCoV solved structure (PDB ID: 6NUR, chain A) is used as a template that shares identical 97.08% of the sequence with COVID-19 RdRp. 6NUR, chain A, is a SARS HCoV non-structural protein 12 (nsp12) solved experimentally using cryo-Electron Microscopy (cryo-EM) with 3.1 Å resolution deposited in the protein data bank last year [35]. The Molprobity web server of the Duke University, and the structure analysis and verification server (SAVES) of the University of California Los Angles (UCLA) are used to test the model [36,37]. The program used to judge the validity of the model are PROCHECK [38], Verify 3D [39], PROVE [40], and ERRAT [41] in addition to the Ramachandran plot of the Molprobity. After validation, the computational chemistry workspace SCIGRESS is used to minimize the model and to perform molecular docking experiments [20,22,42,43]. The minimization of the model is performed using the MM3 force field after the addition of missed Hydrogen atoms [44].

2.2. Molecular docking

Docking experiment is performed using the optimized COVID-19 and SARS (PDB ID: 6NUR, chain A) RdRps by the aid of AutoDock Vina software implemented in SCIGRESS [45]. Eight different compounds

are tested against Wuhan COVID-19 RdRp, including Sofosbuvir, IDX-184, Ribavirin, Remdisivir, Guanosine triphosphate (GTP), Uracil triphosphate (UTP), Cinnamaldehyde, and Thymoquinone. Sofosbuvir is an approved drug by the Food and Drugs Administration (FDA) against Hepatitis C Virus (HCV) Non-structural protein 5 (NS5B) RdRp in the year 2013 [19,46–48]. It gives excellent results against other viruses including the Zika virus [16,17,49,50]. IDX-184 was under clinical trials against HCV and gave better results compared to other drugs against HCV, MERS and SARS HCoVs, and Zika virus RdRps (2017, [11,19,23,51–53]). Ribavirin is a broad-acting antiviral drug used to treat different viruses in combination with immunomodulators or direct-acting antivirals [54–56]. Remdisivir is a nucleotide analog used to treat Ebola virus, Marburg virus, MERS and SARS infections [57]. Cinnamaldehyde and Thymoquinone are negative control compounds that proved its inactivity against RdRp in HCV and Zika virus [26].

After docking, the structures are examined by the aid of the Protein-Ligand Interaction Profiler (PLIP) web server (Technical University of Dresden) and tabulated for comparison [58].

3. Results and discussion

3.1. COVID-19 RdRp modeling

Fig. 1A shows the multiple sequence alignment (MSA) of RNA dependent RNA polymerases from Different HCoV strains including the *Alphacoronaviruses* (229E and NL63) and the *Betacoronaviruses* (OC43, HKU1, SARS, MERS, and COVID-19). SARS HCoV secondary structure is shown at the top of the MSA (PDB ID: 6NUR chain: A) while its water accessibility found at the bottom of the MSA. Highly accessible residues are in blue boxes, while buried residues are represented in white at the bottom of the MSA. The black-dashed rectangle marks active site residues (successive aspartates residues D255 and D256). The active site aspartates are protruding from the beta-turn joining the β15 and β16. As implied from the MSA, the active site is highly conserved (highlighted in red). Also, the 5 Å region surrounding the D255 and D256 is highly conserved in all HCoVs, as shown by the blue-dashed rectangles. This region includes Y114, C117, N186, N190, M251, I252, L253, S254, A257, V258, E306, F307, C308, and S309. The active site residues and most of the 5 Å region surrounding it are surface accessible, though can bind to the free nucleotides (ATP, GTP, CTP, and UTP) [23,25].

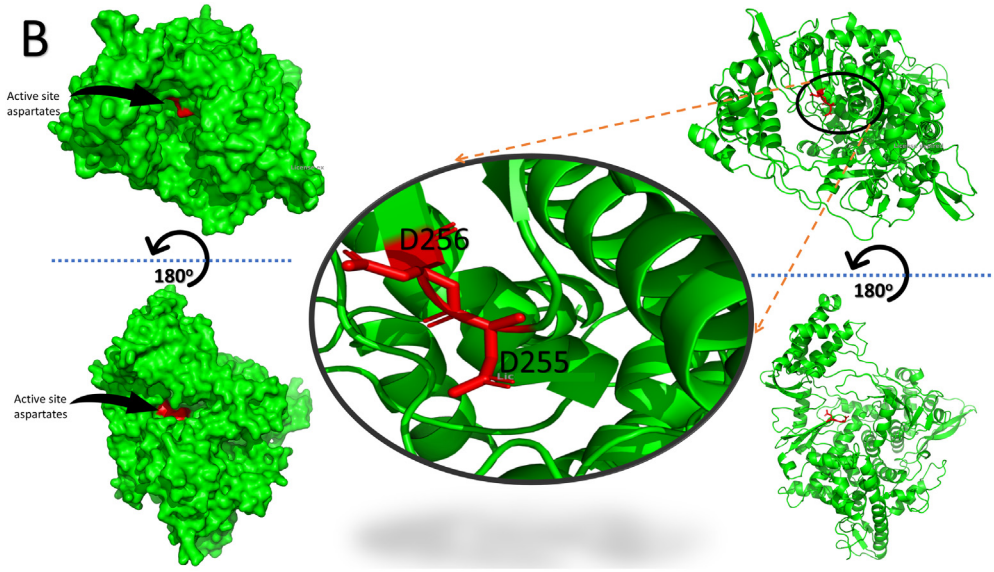

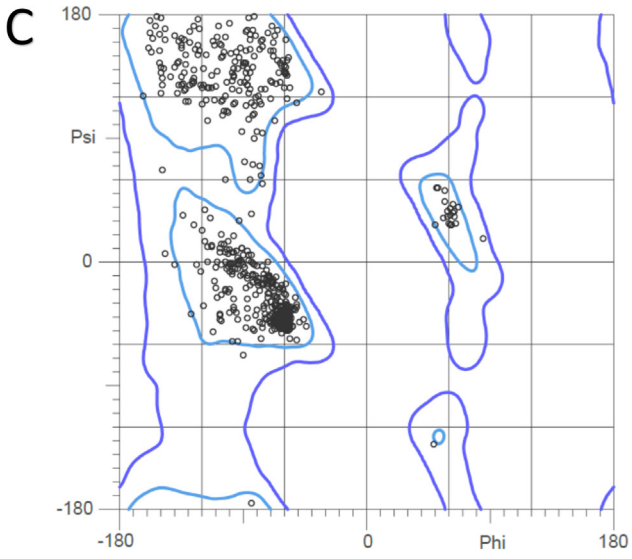

Fig. 1. (*continued*)

Fig. 1B shows the structure of the COVID-19 RdRp model in the green ribbon (right) and green surface (left) representations. Active site residues D255 and D256 are in red for clarification (see the enlarged panel at the center of the figure). The active site is surface accessible as we can see from the surface representation allowing the interaction with the free nucleotides passing through the nucleotide channel of the RdRp. Although some insertions found in COVID-19 RdRp, these insertions are apart from the active site aspartates and have little effect on the model quality (see the Ramachandran plot). Additionally, the homology built model is minimized using the MM3 force field to ensure its reliability before performing the docking study.

For COVID-19 RdRp the percent sequence identity against SARS, MERS, OC43, NL63, 229E, and HKU1 HCoV strains are 90.18%, 56.76%, 55.07%, 48.79%, 48.55%, and 48.16%, respectively. Therefore, the SARS HCoV RdRp is the closest strain to the COVID-19. The complete genome for Wuhan SARS-like HCoV has a sequence identity of 89.12% and 82.34% with Bat SARS-like coronavirus isolate *bat-SL-CoVZC45* and SARS coronavirus *ZS-C*, respectively. This information is important for drug designers to find a quick and potent solution against the newly emerged COVID-19 strain.

COVID-19 RdRp model (801 residues) is built by the aid of the automated homology modeling, Swiss Model, web server using SARS HCoV RdRp (PDB ID: 6NUR, chain A) as a homolog. The model has a very high (97.08%) sequence identity to the template suggesting the high-quality model that could be obtained. The model is valid based on the values we obtain from the validation web servers. The Ramachandran plot shows 100% of the residues in the allowed regions, 97.5% in the most favored region (Fig. 1C). Additionally, 89.9% of the residues have averaged 3D-1D score $\leq$ 0.2 based on the Verify 3D software, while the overall quality factor of ERRAT is 95.9%.

3.2. DAA binding to COVID-19 RdRp

Before performing the docking study, the structures of the small molecules (GTP, UTP, Sofosbuvir, IDX-184, Ribavirin, Remdisivir, Cinnamaldehyde, and Thymoquinone) are prepared, ensured to be in the optimized triphosphate form. Optimization is performed using MM3 then PM6 force field after that further optimization is accomplished through B3LYP functional of Density Functional Theory (DFT) quantum mechanics [44,59–61]. The active site aspartates D255 and D256 are treated as flexible during the docking experiment. A grid box size of 30 × 30 × 30 Å centered at (x, y, z) of (142.1, 138.7, 150.0) Å is used in the docking by utilizing the AutoDock tools [62]. AutoDock Vina utilizes its scoring function (Vina) to predict the interaction between the abovementioned ligands and the RdRps' active site. Fig. 2 shows the docking score values for COVID-19 (blue columns) and SARS HCoVs (orange columns). The SARS solved structure (PDB ID: 6NUR, chain A) is used to dock the same ligands in order to compare its binding energy to that of COVID-19 RdRp. The grid box (30 × 30 × 30 Å) for SARS RdRp is centered at (141.2, 138.5, 149.4) Å. As reflected from the docking scores, the eight compounds, including the physiological GTP and UTP and the four drugs IDX-184, Sofosbuvir, Ribavirin, and Remidisvir can bind to both COVID-19 and SARS HCoV RdRps with good binding energy (−6.5 up to −9.0 kcal/mol). Despite SARS HCoV RdRp show slightly higher binding energies (lower in binding) compared to COVID-19 RdRp, the difference is still non-significant for Ribavirin, Remdisivir, Sofosbuvir and its parent nucleotide, UTP. On average, 0.95 kcal/mol is the difference between the SARS and COVID-19 RdRps' binding energies for these compounds. On the other hand, the difference between COVID-19 and SARS HCoV RdRps' binding energies to IDX-184 and its parent nucleotide GTP are 2.3 and 1.6 kcal/mol, respectively. Additionally, all the tested compounds show lower (better) binding energies to COVID-19 RdRp compared to SARS RdRp. The negative control compounds Cinnamaldehyde and Thymoquinone both show lower binding affinities to either SARS or COVID-19 (higher than −5.6 kcal/mol).

In order to check the possible reason for the differences in the binding energies, we examined the interaction complexes formed after docking by the aid of the PLIP web server. Fig. 3 shows the formed interactions between the DAA drugs and COVID-19 RdRp after docking. The docking scores are listed under each complex to reflect the binding potency. Ligands are shown in orange sticks, while protein residues are in cyan stick representations labeled with its one-letter code. H-bonds are solid blue lines, while the dashed lines represent the hydrophobic interactions. Only one salt bridge (yellow spheres connected by a dashed line) is formed in the case of IDX-184 with D514, which is responsible for the increased stabilization of the formed complex, reflected on the docking score. The number of H-bonds for IDX-184, Sofosbuvir and Ribavirin are 11, 7, and 13, respectively. On the other hand, IDX-184 and Sofosbuvir both form metal interaction through the Mg^{+2} with D652 (two interactions) and E702, respectively. This is another reason for the increased stabilization of the formed complexes for IDX-184 and Sofosbuvir. Additionally, Sofosbuvir formed two hydrophobic interactions with Y510 and D651 of the COVID-19 RdRp.

To summarize the abovementioned data, we can say that IDX-184, Sofosbuvir, and Ribavirin can tightly bind to the newly emerged coronavirus RdRp and hence contradict the function of the protein leading to viral eradication. Additionally, IDX-184 show more promising results

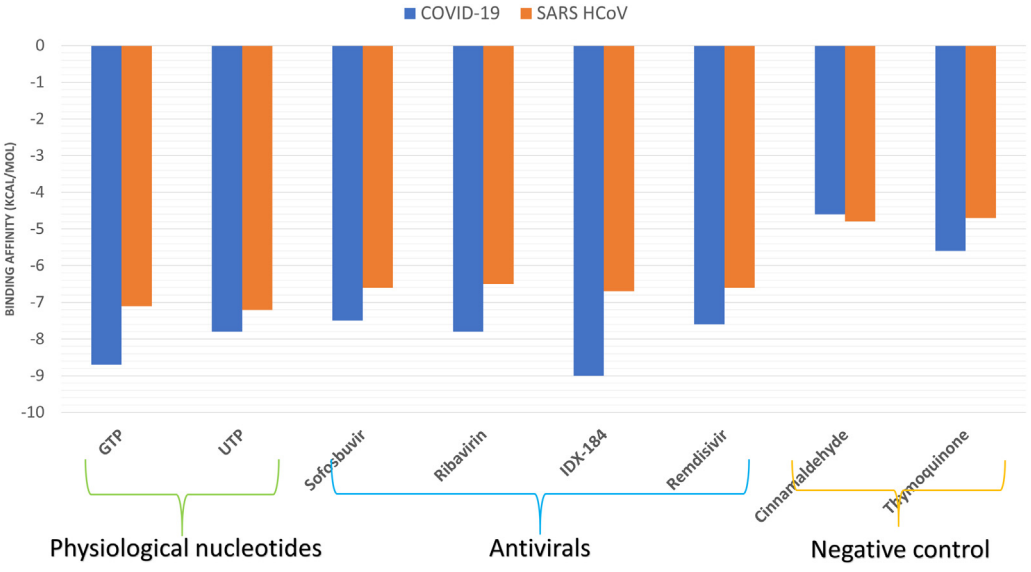

Fig. 2. Binding energies calculated by AutoDock Vina for GTP, UTP, IDX-184, Sofosbuvir, Ribavirin, Remdisivir, Cinnamaldehyde, and Thymoquinone against COVID-19 (blue) and SARS HCoV (orange) RdRps. (For interpretation of the references to color in this figure legend, the reader is referred to the web version of this article.)

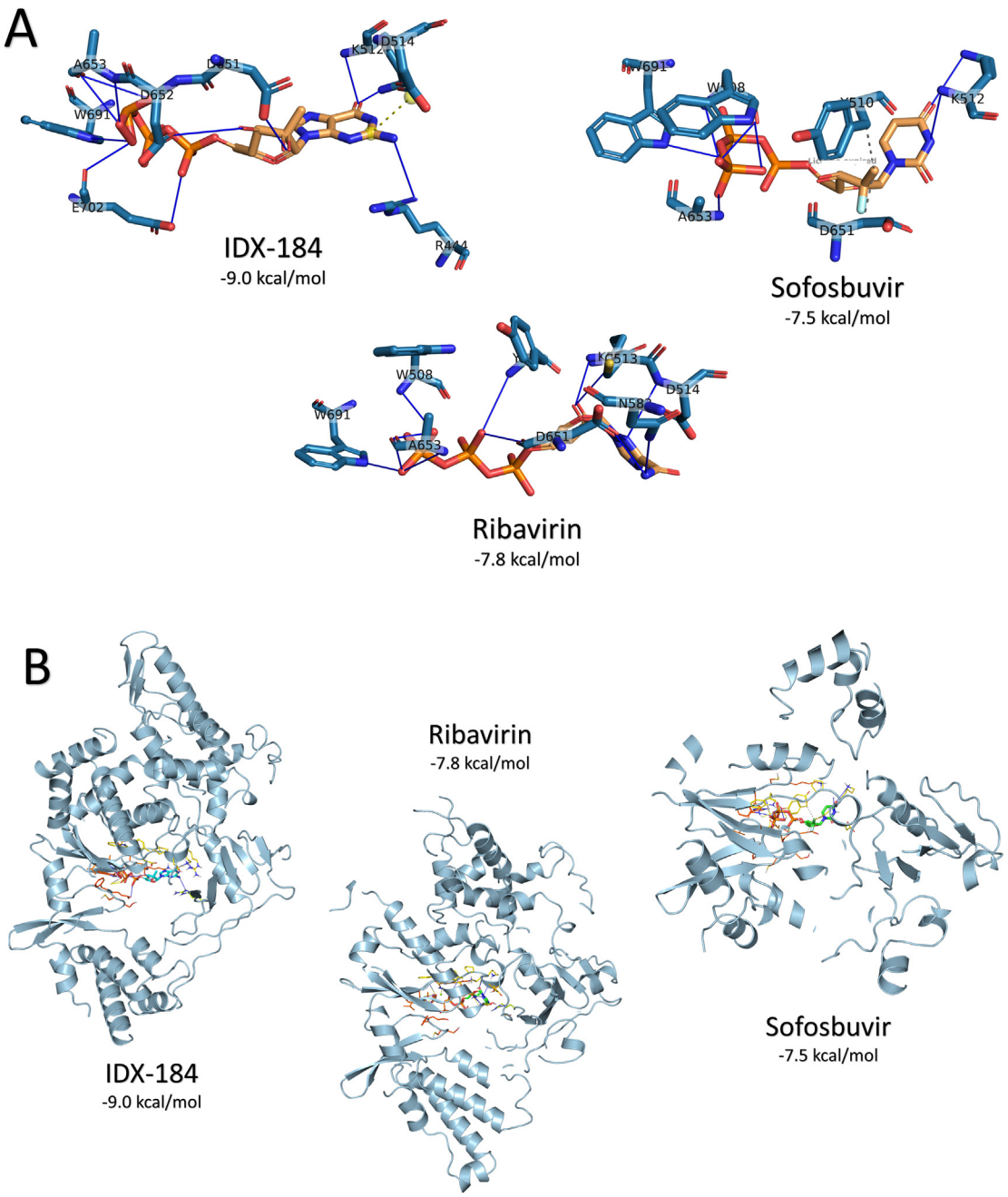

Fig. 3. (A) The interactions that established after docking the DAA drugs IDX-184, Sofosbuvir, and Ribavirin against COVID-19 RdRp are presented. DAAs are in orange while the protein active site pocket in cyan sticks. H-bonds in solid blue lines while hydrophobic interactions are in dashed lines. Salt bridges are in yellow spheres connected by dashed lines. Its one-letter code labels RdRp residues, and the docking scores are listed under each complex. (B) The overall 3D structure complexes arranged as (A). Protein is represented in ribbon, and ligands are in sticks while the interacting residues of the RdRp are represented in colored lines. (For interpretation of the references to color in this figure legend, the reader is referred to the web version of this article.)

then comes Sofosbuvir as a potent inhibitor against the newly emerged COVID-19 strain of HCoV. Further optimization of these two compounds can result in a more potent compound able to stop the newly emerged infection.

4. Conclusion

The newly emerged coronavirus in Wuhan city in China has a health concern since the last outbreak of these types of viruses (SARS) in the year 2002–2003 in the same country leaving > 700 deaths and 8000 cases in hospitals. Besides, another outbreak in the Middle East region has an entirely different infection pattern (MERS) leaving > 800 deaths and 2500 hospitalizations. The present study aimed to test and suggest possible inhibitors, DAA drugs, currently in the market stop the infection immediately. Sofosbuvir, Ribavirin, and Remdisivir can be used against the new strain of coronavirus that emerged with promising results. GTP derivatives may be used as specific inhibitors against COVID-19.

Data availability

The docking structures are available upon request from the corresponding author.

Declaration of competing interest

The author declares that there is no competing interest in this work.

References

[1] I.I. Bogoch, A. Watts, A. Thomas-Bachli, C. Huber, M.U.G. Kraemer, K. Khan, Pneumonia of unknown etiology in Wuhan, China: potential for international spread via commercial air travel, Journal of Travel Medicine (2020).
[2] D.S. Hui, I.E. Azhar, T.A. Madani, F. Ntoumi, R. Kock, O. Dar, et al., The continuing 2019-nCoV epidemic threat of novel coronaviruses to global health—the latest 2019 novel coronavirus outbreak in Wuhan, China, International Journal of Infectious Diseases 91 (2020) 264–266.
[3] Organization WH, Surveillance Case Definitions for Human Infection With Novel Coronavirus (nCoV): Interim Guidance v1, January 2020, World Health Organization, 2020.
[4] Organization WH, Infection Prevention and Control during Health Care When Novel Coronavirus (nCoV) Infection Is Suspected: Interim Guidance, January 2020, World Health Organization, 2020.
[5] Organization WH, Laboratory Testing of Human Suspected Cases of Novel Coronavirus (nCoV) Infection: Interim Guidance, 10 January 2020, World Health Organization, 2020.
[6] J. Parr, Pneumonia in China: Lack of Information Raises Concerns Among Hong Kong Health Workers, British Medical Journal Publishing Group, 2020.
[7] A.A.I. Elfiky, N. S, Anti-SARS and Anti-HCV Drugs Repurposing Against the Papain-like Protease of the Newly Emerged Coronavirus (2019-nCoV), preprint (2020).
[8] I.M.A. Ibrahim, D.H. Elshahat, M.M. Elfiky, A. Abdo, COVID-19 Spike-host Cell Receptor GRP78 Binding Site Prediction, preprint (2020).
[9] L. Yang, China Confirms Human-to-Human Transmission of Coronavirus, (2020).
[10] J.F. Chan, S.K. Lau, K.K. To, V.C. Cheng, P.C. Woo, K.-Y. Yuen, Middle East respiratory syndrome coronavirus: another zoonotic betacoronavirus causing SARS-like disease, Clin. Microbiol. Rev. 28 (2015) 465–522.
[11] A.A. Elfiky, S.M. Mahdy, W.M. Elshemey, Quantitative structure-activity relationship and molecular docking revealed a potency of anti-hepatitis C virus drugs against human corona viruses, J. Med. Virol. 89 (2017) 1040–1047.
[12] WHO, Middle East Respiratory Syndrome Coronavirus (MERS-CoV), WHO, 2016.
[13] Y.M. Báez-Santos, A.M. Mielech, X. Deng, S. Baker, A.D. Mesecar, Catalytic function and substrate specificity of the papain-like protease domain of nsp3 from the Middle East respiratory syndrome coronavirus, J. Virol. 88 (2014) 12511–12527.
[14] M.G. Hemida, A. Alnaeem, Some one health based control strategies for the Middle East respiratory syndrome coronavirus, One Health. 8 (2019) 100102.
[15] Organization WH, Clinical Management of Severe Acute Respiratory Infection When Middle East Respiratory Syndrome Coronavirus (MERS-CoV) Infection Is Suspected: Interim Guidance, World Health Organization, 2019.
[16] A.A. Elfiky, Zika viral polymerase inhibition using anti-HCV drugs both in market and under clinical trials, J. Med. Virol. 88 (2016) 2044–2051.
[17] A.A. Elfiky, Zika virus: novel guanosine derivatives revealed strong binding and possible inhibition of the polymerase, Futur. Virol. 12 (2017) 721–728.
[18] A.A. Elfiky, Novel guanosine derivatives as anti-HCV NS5b polymerase: a QSAR and molecular docking study, Med. Chem. 15 (2019) 130–137.
[19] A.A. Elfiky, W.M. Elshemey, IDX-184 is a superior HCV direct-acting antiviral drug: a QSAR study, Med. Chem. Res. 25 (2016) 1005–1008.
[20] A.A. Elfiky, W.M. Elshemey, Molecular dynamics simulation revealed binding of nucleotide inhibitors to ZIKV polymerase over 444 nanoseconds, J. Med. Virol. 90 (2018) 13–18.
[21] A.A. Elfiky, W.M. Elshemey, W.A. Gawad, O.S. Desoky, Molecular modeling comparison of the performance of NS5b polymerase inhibitor (PSI-7977) on prevalent HCV genotypes, Protein J. 32 (2013) 75–80.
[22] A.A. Elfiky, A. Ismail, Molecular dynamics and docking reveal the potency of novel GTP derivatives against RNA dependent RNA polymerase of genotype 4a HCV, Life Sci. 238 (2019) 116958.
[23] A.A. Elfiky, A.M. Ismail, Molecular modeling and docking revealed superiority of IDX-184 as HCV polymerase inhibitor, Futur. Virol. 12 (2017) 339–347.
[24] A. Ganesan, K. Barakat, Applications of computer-aided approaches in the development of hepatitis C antiviral agents, Expert Opin. Drug Discovery 12 (2017) 407–425.
[25] S. Doublie, T. Ellenberger, The mechanism of action of T7 DNA polymerase, Curr. Opin. Struct. Biol. 8 (1998) 704–712.
[26] A.A. Elfiky, A.M. Ismail, Molecular docking revealed the binding of nucleotide/side inhibitors to Zika viral polymerase solved structures, SAR QSAR Environ. Res. 29 (2018) 409–418.
[27] A.A. Ezat, A.A. Elfiky, W.M. Elshemey, N.A. Saleh, Novel inhibitors against wild-type and mutated HCV NS3 serine protease: an in silico study, VirusDisease. 30 (2) (2019) 207–213.
[28] P.L. Yang, M. Gao, K. Lin, Q. Liu, V.A. Villareal, Anti-HCV drugs in the pipeline, Curr Opin Virol. 1 (2011) 607–616.
[29] W. Markland, T. McQuaid, J. Jain, A. Kwong, Broad-spectrum antiviral activity of the IMP dehydrogenase inhibitor VX-497: a comparison with ribavirin and demonstration of antiviral additivity with alpha interferon, Antimicrob. Agents Chemother. 44 (2000) 859–866.
[30] M. Wang, R. Cao, L. Zhang, X. Yang, J. Liu, M. Xu, et al., Remdesivir and chloroquine effectively inhibit the recently emerged novel coronavirus (2019-nCoV) in vitro, Cell Res. (2020) 1–3.
[31] T. McQuaid, C. Savini, S. Seyedkazemi, Sofosbuvir, a significant paradigm change in HCV treatment, J Clin Transl Hepatol. 3 (2015) 27–35.
[32] H. Berman, K. Henrick, H. Nakamura, Announcing the worldwide Protein Data Bank, Nat Struct Mol Biol. 10 (2003) 980–.
[33] NCBI, National Center of Biotechnology Informatics (NCBI) database website, http://www.ncbi.nlm.nih.gov/, (2020).
[34] M. Biasini, S. Bienert, A. Waterhouse, K. Arnold, G. Studer, T. Schmidt, et al., SWISS-MODEL: modelling protein tertiary and quaternary structure using evolutionary information, Nucleic Acids Res. 42 (2014) W252-W8.
[35] R.N. Kirchdoerfer, A.B. Ward, Structure of the SARS-CoV nsp12 polymerase bound to nsp7 and nsp8 co-factors, Nat. Commun. 10 (2019) 2342.
[36] SAVES, Structural Analysis and Verification Server Website, (2020).
[37] C.J. Williams, J.J. Headd, N.W. Moriarty, M.G. Prisant, L.L. Videau, L.N. Deis, et al., MolProbity: more and better reference data for improved all-atom structure validation, Protein Sci. 27 (2018) 293–315.
[38] R.A. Laskowski, J.A.C. Rullmann, M.W. MacArthur, R. Kaptein, J.M. Thornton, AQUA and PROCHECK-NMR: programs for checking the quality of protein structures solved by NMR, J. Biomol. NMR 8 (1996) 477–486.
[39] D. Eisenberg, R. Lüthy, J.U. Bowie, VERIFY3D: assessment of protein models with three-dimensional profiles, Methods in Enzymology: Elsevier (1997) 396–404.
[40] J. Pontius, JRaSJW, Deviations from standard atomic volumes as a quality measure for protein crystal structures, Journal of Molecular Biology 264 (1996) 121–136.
[41] R.W. Hooft, G. Vriend, C. Sander, E.E. Abola, Errors in protein structures, Nature. 381 (1996) 272.
[42] A.A. Elfiky, The antiviral Sofosbuvir against mucormycosis: an in silico perspective, Future Virology 0 (2020) null.
[43] K.L. Summers, A.K. Mahrok, M.D. Dryden, M.J. Stillman, Structural properties of metal-free apometallothioneins, Biochem. Biophys. Res. Commun. 425 (2012) 485–492.
[44] J.H. Lii, N.L. Allinger, Molecular mechanics. The MM3 force field for hydrocarbons. 3. The van der Waals' potentials and crystal data for aliphatic and aromatic hydrocarbons, J. Am. Chem. Soc. 111 (1989) 8576–8582.
[45] O. Trott, A.J. Olson, AutoDock Vina: improving the speed and accuracy of docking with a new scoring function, efficient optimization, and multithreading, J. Comput. Chem. 31 (2010) 455–461.
[46] M. Angela, C.E. Lam, S. Bansal, H.M. Micolochick Steuer, C. Niu, V. Zennou, M. Keilman, Y. Zhu, S. Lan, M.J. Otto, P.A. Furman, Genotype and subtype profiling of PSI-7977 as a nucleotide inhibitor of hepatitis C virus, Antimicrob. Agents Chemother. 56 (2012) 3359–3368.
[47] A.A. Elfiky, A. GW, M. EW, A. M, Hepatitis C viral polymerase inhibition using directly acting antivirals, a computational approach, Software and Techniques for Bio-Molecular Modeling, Austin Publishing Group, USA, 2016, p. 197.
[48] M.J.O. Lam, M.J. Sofia, C. Espiritu, S. Bansal, A.M. Steuer, D. Bao, W. Chang, C.N. Bao, H.M. Micolochick Eisuke Murakami, T. Tolstykh, H.P.A. Furman, Mechanism of activation of PSI-7851 and its diastereoisomer PSI-7977, J. Biol. Chem. 285 (2010) 34337–34347.
[49] K.M. Bullard-Feibelman, J. Govero, Z. Zhu, V. Salazar, M. Veselinovic, M.S. Diamond, et al., The FDA-approved drug sofosbuvir inhibits Zika virus infection, Antivir. Res. 137 (2017) 134–140.
[50] C.Q. Sacramento, G.R. de Melo, N. Rocha, H. LVB, M. Mesquita, C.S. de Freitas, et al., The clinically approved antiviral drug sofosbuvir impairs Brazilian zika virus replication, Sci Rep. 7 (2017) 40920, https://doi.org/10.1038/srep40920.
[51] E. Cretton-Scott, C. Perigaud, S. Peyrottes, L. Licklider, M. Camire, M. Larsson, et al., 588 in vitro antiviral activity and pharmacology of IDX184, a novel and potent inhibitor of HCV replication, J. Hepatol. 48 (2008) S220.
[52] A.A. Elfiky, W.M. Elshemey, W.A. Gawad, 2′-Methylguanosine prodrug (IDX-184), phosphoramidate prodrug (Sofosbuvir), diisobutyryl prodrug (R7128) are better than their parent nucleotides and ribavirin in hepatitis C virus inhibition: a molecular modeling study, J. Comput. Theor. Nanosci. 12 (2015) 376–386.
[53] X.J. Zhou, K. Pietropaolo, J. Chen, S. Khan, J. Sullivan-Bolyai, D. Mayers, Safety and pharmacokinetics of IDX184, a liver-targeted nucleotide polymerase inhibitor of hepatitis C virus, in healthy subjects, Antimicrob. Agents Chemother. 55 (2011) 76–81.
[54] E.J. Gane, C.A. Stedman, R.H. Hyland, X. Ding, E. Svarovskaia, W.T. Symonds, et al., Nucleotide polymerase inhibitor sofosbuvir plus ribavirin for hepatitis C, N. Engl. J. Med. 368 (2013) 34–44.
[55] P. Glue, The Clinical Pharmacology of Ribavirin. Seminars in Liver Disease, (1999), pp. 17–24.
[56] M.P. Manns, J.G. McHutchison, S.C. Gordon, V.K. Rustgi, M. Shiffman, R. Reindollar, et al., Peginterferon alfa-2b plus ribavirin compared with interferon alfa-2b plus ribavirin for initial treatment of chronic hepatitis C: a randomised trial, Lancet 358 (2001) 958–965.
[57] T.K. Warren, R. Jordan, M.K. Lo, A.S. Ray, R.L. Mackman, V. Soloveva, et al., Therapeutic efficacy of the small molecule GS-5734 against Ebola virus in rhesus monkeys, Nature. 531 (2016) 381–385.
[58] S. Salentin, S. Schreiber, V.J. Haupt, M.F. Adasme, M. Schroeder, PLIP: fully automated protein–ligand interaction profiler, Nucleic Acids Res. 43 (2015) W443-W7.
[59] A.D. Becke, Density-functional thermochemistry. III. The role of exact exchange, J. Chem. Phys. 98 (1993) 5648–5652.
[60] A. Leach, Molecular Modelling: Principles and Applications, 2nd edition, Prentice Hall, 2001.
[61] J.J.P. Stewart, Optimization of parameters for semiempirical methods V: modification of NDDO approximations and application to 70 elements, J. Mol. Model. 13 (2007) 1173–1213.
[62] G.M. Morris, R. Huey, W. Lindstrom, M.F. Sanner, R.K. Belew, D.S. Goodsell, et al., AutoDock4 and AutoDockTools4: automated docking with selective receptor flexibility, J. Comput. Chem. 30 (2009) 2785–2791.
[63] I. Ibrahim, D. Abdelmalek, M. Elshahat, A. Elfiky, COVID-19 Spike-host cell receptor GRP78 binding site prediction, J. Infect. (2020) In press.